

Mapping the thermal history of the Universe with the new generation of CMB spectrum space experiments

C. Burigana¹ and R. Salvaterra²

¹*IASF/CNR, Istituto di Astrofisica Spaziale e Fisica Cosmica, Sezione di Bologna, Consiglio Nazionale delle Ricerche, Via Gobetti 101, I-40129 Bologna, Italy*

²*SISSA/ISAS, Astrophysics Sector, Via Beirut, 4, I-34014 Trieste, Italy*

Submitted to MNRAS, 12 September 2003.

ABSTRACT

We have studied the implications of the new generation of CMB spectrum space experiments for our knowledge of the thermal history of the Universe.

The combination of two experiments with the sensitivity and the frequency coverage jointly foreseen for *DIMES* and FIRAS II will be able to greatly change our vision of the capability of the CMB spectrum information to constrain physical processes at different cosmic ages. The limits on the energy dissipations at the all cosmic times accessible to CMB spectrum investigations ($z \lesssim z_{therm}$) could be improved by about two order of magnitudes and even dissipation processes with $\Delta\epsilon/\epsilon_i \sim 10^{-6}$ could be detected and possibly accurately studied.

With a joint analysis of two dissipation processes occurring at different epochs, we demonstrated that the joint performances of *DIMES* and FIRAS II would allow to accurately recover the two amounts of energy exchanged in the primeval plasma and to constrain quite well also the epochs of the two processes even when possible imprints from free-free distortions are taken into account. All the three distortion parameters could be accurately reconstructed in this perspective: the sensitivity at 95 per cent CL is $\simeq (5 - 9) \times 10^{-7}$ for the two values of $\Delta\epsilon/\epsilon_i$ and of $\simeq 10^{-7}$ for the free-free distortion parameter y_B . These results are possible because such levels of accuracy on a so wide frequency range allow to remove the approximate degeneracy both between free-free and Bose-Einstein (BE) like distortions and between Comptonization and BE-like distortions that remain in presence of future significant improvements only at $\lambda \gtrsim 1$ cm or at $\lambda \lesssim 1$ cm, respectively. The sensitivity on $\Delta\epsilon/\epsilon_i$, mainly determined by a FIRAS II-like experiment, improves by a factor $\simeq 1.5$ by adding the information from a *DIMES*-like experiment, while the sensitivity on y_B , mainly determined by a *DIMES*-like experiment, improves by a factor $\simeq 1.3 - 2.6$, by adding the information from a FIRAS II-like experiment.

Finally, we discussed the different signatures imprinted on the CMB spectrum by some late astrophysical and particle decay models recently proposed in the literature and possibly related to the reionization of the Universe indicated by *WMAP*, and compared them with the sensitivity of such classes of CMB space spectrum experiments.

Key words: cosmology: cosmic microwave background – cosmology: theory

1 INTRODUCTION

As widely discussed in many papers, the spectrum of the Cosmic Microwave Background (CMB) carries unique informations on physical processes occurring during early cosmic epochs (see e.g. Danese & Burigana 1993 and references therein). The comparison between models of CMB spectral distortions and CMB absolute temperature measures can constrain the physical

parameters of the considered dissipation processes. By jointly considering distortions generated in a wide range of early or intermediate cosmic epochs and at late cosmic epochs, we recently discussed the implications of the current CMB spectrum data (Salvaterra & Burigana 2002) as well as the great improvements in the knowledge of dissipation processes, in particular on those possibly occurred at early and intermediate epochs, achievable with a significant progress in the experiments at long wavelength, $\lambda \gtrsim 1$ cm, (Burigana & Salvaterra 2003), such that expected from a *DIMES*-like project (Kogut 1996, 2003).

Fixsen & Mather (2002) recently proposed a new generation of millimeter and submillimeter spectrum experiment, FIRAS II, aimed to improve by a factor ~ 100 the accuracy of the COBE/FIRAS measures.

While in the last decade many efforts have been ^{*} (see e.g. Bennett et al. 1996, 2003 and references therein) and are currently [†] (see e.g. Mandolesi et al. 1998, Puget et al. 1998, Tauber 2000 and references therein) dedicated to greatly improve our knowledge of the whole sky CMB anisotropies since their COBE/DMR discovery (Smoot et al. 1992), the combination of high precision and large frequency coverage jointly foreseen for *DIMES* and FIRAS II opens a completely new perspective also in CMB spectrum studies, as we will discuss in this paper.

In section 2 we briefly summarize the general properties of the CMB spectral distortions and the main physical informations that can be derived from the comparison with the observations. In section 3 we briefly report on the performances foreseen for the *DIMES* and FIRAS II experiments and describe the generation of the simulated observations used in this work. The implications of such experiments for our knowledge of the thermal history of the Universe are presented in section 4: models including an undistorted spectrum and distorted spectra in the case of a single kind of spectral distortion or by jointly considering three kinds of spectral distortions are compared with data simulated according to the sensitivities quoted for the above experiments (the joint analysis of two spectral distortions is reported in Appendix A for completeness). Section 5 is dedicated to a comparison between some different classes of astrophysical and particle processes recently discussed in the literature occurring at relatively late epochs, able to distort the spectrum at different wavelength regions, and, possibly, to significantly contribute to the reionization of the Universe. Finally, we discuss the results and draw our main conclusions in section 6.

2 THEORETICAL FRAMEWORK

The CMB spectrum emerges from the thermalization redshift, $z_{therm} \sim 10^6 - 10^7$, with a shape very close to a Planckian one, owing to the strict coupling between radiation and matter through Compton scattering and photon production/absorption processes, radiative Compton and Bremsstrahlung, which were extremely efficient at early times and able to re-establish a blackbody (BB) spectrum from a perturbed one on timescales much shorter than the expansion time (see e.g. Danese & De Zotti 1977). The value of z_{therm} (Burigana, Danese & De Zotti 1991a) depends on the baryon density (in units of the critical density), Ω_b , and the Hubble constant, H_0 , through the product $\hat{\Omega}_b = \Omega_b (H_0/50)^2$ (H_0 expressed in Km/s/Mpc).

On the other hand, physical processes occurring at redshifts $z < z_{therm}$ may lead imprints on the CMB spectrum.

The timescale for the achievement of kinetic equilibrium between radiation and matter (i.e. the relaxation time for the photon spectrum), t_C , is

$$t_C = t_{\gamma e} \frac{mc^2}{kT_e} \simeq 4.5 \times 10^{28} (T_0/2.7 K)^{-1} \phi^{-1} \hat{\Omega}_b^{-1} (1+z)^{-4} \text{ sec}, \quad (1)$$

where $t_{\gamma e} = 1/(n_e \sigma_{Te})$ is the photon-electron collision time, $\phi = (T_e/T_r)$, T_e being the electron temperature and $T_r = T_0(1+z)$; kT_e/mc^2 is the mean fractional change of photon energy in a scattering of cool photons off hot electrons, i.e. $T_e \gg T_r$; T_0 is the present radiation temperature related to the present radiation energy density by $\epsilon_{r0} = aT_0^4$; a primordial helium abundance of 25% by mass is here assumed.

It is useful to introduce the dimensionless time variable $y_e(z)$ defined by

$$y_e(z) = \int_t^{t_0} \frac{dt}{t_C} = \int_1^{1+z} \frac{d(1+z)}{1+z} \frac{t_{exp}}{t_C}, \quad (2)$$

where t_0 is the present time and t_{exp} is the expansion time given by

$$t_{exp} \simeq 6.3 \times 10^{19} \left(\frac{T_0}{2.7 K} \right)^{-2} (1+z)^{-3/2} \left[\kappa(1+z) + (1+z_{eq}) - \left(\frac{\Omega_{nr} - 1}{\Omega_{nr}} \right) \left(\frac{1+z_{eq}}{1+z} \right) \right]^{-1/2} \text{ sec}, \quad (3)$$

$z_{eq} = 1.0 \times 10^4 (T_0/2.7 K)^{-4} \hat{\Omega}_{nr}$ being the redshift of equal non relativistic matter and photon energy densities (Ω_{nr} is the density of non relativistic matter in units of critical density); $\kappa = 1 + N_\nu (7/8) (4/11)^{4/3}$, N_ν being the number of relativistic,

^{*} <http://lambda.gsfc.nasa.gov>

[†] <http://astro.estec.esa.nl/Planck/>

2-component, neutrino species (for 3 species of massless neutrinos, $\kappa \simeq 1.68$), takes into account the contribution of relativistic neutrinos to the dynamics of the Universe[‡].

Burigana, De Zotti & Danese 1991b have reported on numerical solutions of the Kompaneets equation (Kompaneets 1956) for a wide range of values of the relevant parameters and accurate analytical representations of these numerical solutions, suggested in part by the general properties of the Kompaneets equation and by its well known asymptotic solutions, have been found (Burigana, De Zotti & Danese 1995).

The CMB distorted spectra depend on at least three main parameters: the fractional amount of energy exchanged between matter and radiation, $\Delta\epsilon/\epsilon_i$, ϵ_i being the radiation energy density before the energy injection, the redshift z_h at which the heating occurs, and the baryon density $\hat{\Omega}_b$. The photon occupation number can be then expressed in the form

$$\eta = \eta(x; \Delta\epsilon/\epsilon_i, y_h, \hat{\Omega}_b), \quad (4)$$

where x is the dimensionless frequency $x = h\nu/kT_0$ (ν being the present frequency), and $y_h \equiv y_e(z_h)$ characterizes the epoch when the energy dissipation occurred, z_h being the corresponding redshift (we will refer to $y_h \equiv y_e(z_h)$ computed assuming $\phi = 1$, so that the epoch considered for the energy dissipation does not depend on the amount of released energy). The continuous behaviour of the distorted spectral shape with y_h can be in principle used also to search for constraints on the epoch of the energy exchange. Of course, by combining the approximations describing the distorted spectrum at early (Sunyaev & Zeldovich 1970) and intermediate epochs with the Comptonization distortion expression (Zeldovich & Sunyaev 1969; Zeldovich, Illarionov & Sunyaev 1972) describing late distortions, it is possible to jointly treat two heating processes (see Burigana et al. 1995 and Salvaterra & Burigana 2002 and references therein for a more exhaustive discussion).

In this work simulated measures of the CMB absolute temperature are compared with the above models of distorted spectra by using a standard χ^2 analysis.

We determine the limits on the amount of energy possibly injected in the cosmic background at arbitrary primordial epochs corresponding to a redshift z_h (or equivalently to y_h). This topic has been discussed in several works (see e.g. Burigana et al. 1991b, Nordberg & Smoot 1998, Salvaterra & Burigana 2002). We apply here the method of comparison with the theoretical models described in Salvaterra & Burigana 2002 and Burigana & Salvaterra 2003, by investigating the possibility of properly combining data simulated according to the *DIMES* and *FIRAS* II performances respectively at long and short wavelengths.

We will consider the recent improvement in the calibration of the *FIRAS* data, that sets the CMB scale temperature at 2.725 ± 0.002 K at 95 per cent confidence level (CL) (Mather et al. 1999).

Then, we study the combined effect of two different heating processes that may have distorted the CMB spectrum at different epochs. This hypothesis has been also taken into account by Nordberg & Smoot 1998, who fit the observed data with a spectrum distorted by a single heating at $y_h = 5$, a second one at $y_h \ll 1$ and by free-free emission, obtaining limits on the parameters that describe these processes. As in Salvaterra & Burigana 2002, we extend their analysis by considering the full range of epochs for the early and intermediate energy injection process, by taking advantage of the analytical representation of spectral distortions at intermediate redshifts (Burigana et al. 1995).

Long wavelength measures are particularly sensitive to the free-free distortion due to its well known dependence on the frequency. At moderately long wavelengths, where quite accurate observations can be carried out, $(T_{th} - T_0\phi_i)/T_0 \simeq y_B/x^2$. Here ϕ_i is the ratio between the electron and radiation temperature before the beginning of the dissipation process, y_B is the so called free-free distortion parameter (Burigana et al. 1995), and T_{th} is the (frequency dependent) equivalent thermodynamic temperature. At very long wavelengths the equivalent thermodynamic temperature approaches the electron temperature because of the very high bremsstrahlung efficiency.

The relationship between free-free distortion and Comptonization distortion is highly model dependent, being related to the details of the thermal history at late epochs (see e.g. Danese & Burigana 1993, Burigana et al. 1995), and can not be simply represented by integral parameters.

In the combined analysis of the implications of future CMB spectrum experiments for energy dissipations at different cosmic times and free-free distortions we avoid to physically link Comptonization and free-free distortions. Eq. (4) generalizes then to

$$\eta = \eta(x; \Delta\epsilon/\epsilon_i(y_h), y_h, \Delta\epsilon/\epsilon_i(y_h \ll 1), y_B, \hat{\Omega}_b). \quad (5)$$

Comptonization and free-free emission could be also produced in several astrophysical scenarios. For example, ionized halos in the early stages of galaxy formation (Oh 1999) can produce a relevant free-free distortions and coupled Comptonization and free-free distortions can be produced in the reionization epoch, indicated by the *WMAP* data (Kogut et al. 1993).

It is also possible to extend the limits on $\Delta\epsilon/\epsilon_i$ for heatings occurred at $z_h > z_1$, where z_1 is the redshift corresponding to

[‡] Strictly speaking the present ratio of neutrino to photon energy densities, and hence the value of κ , is itself a function of the amount of energy dissipated. The effect, however, is never very important and is negligible for very small distortions.

$y_h = 5$, when the Compton scattering was able to restore the kinetic equilibrium between matter and radiation on timescales much shorter than the expansion time and the evolution on the CMB spectrum can be easily studied by replacing the full Kompaneets equation with the differential equations for the evolution of the electron temperature and the chemical potential. This study can be performed by using the simple analytical expressions by Burigana et al. 1991b instead of numerical solutions.

To evaluate the scientific impact represented by the future experiment improvements, we create different data sets simulating the observation of a distorted and non distorted spectra from a space experiments like *DIMES* and FIRAS II through the method described in section 3.1.

Each data set will be then compared to models of distorted spectra by using the method described in Salvaterra & Burigana 2002 (see also Burigana & Salvaterra 2000 for the details of the code) to recover the values of the parameters appearing in Eq. (5).

For simplicity, we restrict to the case of a baryon density $\hat{\Omega}_b = 0.05$ our analysis of the implications for the thermal history of the Universe, but the method can be simply applied to different values of $\hat{\Omega}_b$.

3 FUTURE EXPERIMENTS

The CMB spectrum experiments considered here are dedicated to improve our knowledge both at the same and at longer wavelengths with respect to the FIRAS frequency coverage ($1 \text{ cm} \gtrsim \lambda \gtrsim 0.01 \text{ cm}$).

As representative cases, and without the ambition to cover the whole set of planned experiments, we briefly refer here to the *DIMES* experiment from space (Kogut 1996) designed to reach an accuracy close to that of FIRAS up to $\lambda \simeq 15 \text{ cm}$ and to the FIRAS II experiment (Fixsen & Mather 2002) which will allow a sensitivity improvement by a factor ~ 100 with respect to FIRAS.

DIMES[§] (Diffuse Microwave Emission Survey) is a space mission submitted to the NASA in 1995, designed to measure very accurately the CMB spectrum at wavelengths in the range $\simeq 0.5 - 15 \text{ cm}$ (Kogut 1996).

DIMES will compare the spectrum of each 10 degree pixel on the sky to a precisely known blackbody to precision of $\sim 0.1 \text{ mK}$, close to that of FIRAS ($\simeq 0.02 - 0.2 \text{ mK}$). The set of receivers is given from cryogenic radiometers with instrument emission cooled to 2.7 K operating at six frequency bands about 2, 4, 6, 10, 30 and 90 GHz using a single external blackbody calibration target common to all channels to minimize the calibration uncertainty. The *DIMES* design is driven by the need to reduce or eliminate systematic errors from instrumental artifacts. The *DIMES* sensitivity represents an improvement by a factor better than 300 with respect to previous measurements at cm wavelengths.

Fixsen & Mather (2002) described the fundamental guidelines to significantly improve CMB spectrum measures at $\lambda \lesssim 1 \text{ cm}$. A great reduction of the residual noise of cosmic rays, dominating the noise of the FIRAS instrument, can be obtained by eliminating the data on-board co-add process or applying deglitching before co-adding, by reducing the size of the detectors and by using “spiderweb” bolometers or antenna-coupled microbolometers. They are expected to show a very low noise when cooled below 1 K while RuO sensors can reduce to 0.1 mK the read noise of thermometers. The Lagrangian point L2 of the Earth-Sun system is, of course, the favourite “site” for FIRAS II. Also, the calibration can be improved by order of magnitudes with respect to that FIRAS by reducing the contribution to the calibrator reflectance of light from the diffraction at the junction between the calibrator and the horn. A complete symmetrical construction of the instrument is recommended. This allows the cross-check between calibrators and between calibrators and the sky and to realize “an end-to-end calibration and performance test before lunch”. According to the authors, FIRAS II can be designed to have a frequency coverage from 60 to 3600 GHz (i.e. from 5 mm to 83 μm) with a spectral resolution $\nu/\Delta\nu < 200$ and sensitivity in each channel about 100 times better than FIRAS.

3.1 Generation of simulated data sets

We collect different data sets, simulating measurements of different CMB spectra, distorted or not, at the frequency ranges of the considered experiments.

For the cases of distorted spectra we calculate the theoretical temperature of the CMB spectrum as discussed in the previous section. Of course, the equivalent thermodynamic temperature held obviously constant at all the frequencies for the case of a non distorted spectrum.

The theoretical temperatures are then fouled to simulate real measurements affected by instrumental noise. The simulated temperature T_{obs} at the frequency ν is given by $T_{obs}(\nu) = T_{teor}(\nu) + n(\nu) \times \text{err}(\nu)$, where $T_{teor}(\nu)$ is the theoretical temperature at the frequency ν and $\text{err}(\nu)$ is the expected rms error (at 1σ) of the experiment at this frequency. The numbers n are a set

[§] <http://map.gsfc.nasa.gov/DIMES/index.html>

of random numbers generated according to a Gaussian distribution with null mean value and unit variance with the routine GASDEV by Press et al. 1992 (§7).

The considered frequency channels are those of *DIMES* and those achievable with the spectral resolution foreseen for FIRAS II. For sake of simplicity and differently from the analysis carried out in Salvaterra & Burigana 2002, we do not consider here the wavelength region at $\lambda \leq 800\mu\text{m}$, accessible to FIRAS II, and neglect the problem of separating the signatures of CMB spectral distortions, dominant at $\lambda \gtrsim 1\text{ mm}$, from the contribution from Far-IR galaxies, dominant at $\lambda \lesssim 500\mu\text{m}$.

3.2 Simulated data sets

We generate a set (S-BB) of simulated data in the case of a blackbody spectrum at a temperature of 2.725 K in order to evaluate the joint capability of two experiments like *DIMES* and FIRAS II to improve the constraints on the amount of the energy injected in the cosmic radiation field. The analysis of this case is in fact directly comparable with the results obtained from the fit to the currently available data.

Of course, it is extremely important to evaluate the capability of so accurate experiments to detect and, possibly, precisely measure the spectral distortion parameters, the fractional energy exchanges and the dissipation epochs. To this aim, we generate other three sets of simulated data (respectively, S-E5C, S-E1.5C, S-E0.1C) assuming an instantaneous ($\delta y_h \ll y_h$) earlier energy dissipation with $\Delta\epsilon/\epsilon_i(y_h) = 3 \times 10^{-6}$ ($\simeq \mu/1.4$, where μ is the chemical potential of the Bose-Einstein (BE) formula describing the high frequency tail of the spectrum for distortions at sufficiently high redshifts) occurring at $y_h = 5$ or at $y_h = 1.5$ or at $y_h = 0.1$ plus a later Comptonization distortion associated to an energy dissipation $\Delta\epsilon/\epsilon_i(y_h \ll 1) = 3 \times 10^{-6} \simeq 4u$ (here u is the “energy” Comptonization parameter). For simplicity, we assume here $y_B = 0$ (see Sect. 5 for a discussion of combined Comptonization and free-free distortions on the basis of some specific models). All these distorted spectra are computed by setting $\Omega_b = 0.05$ and $H_0 = 50\text{ Km/s/Mpc}$.

These above simulated data set will be compared with models including spectral distortions generated by a dissipation process occurred at very different cosmic epochs, on a grid represented by the dimensionless time $y_h = 5, 4, 3, 2, 1, 0.5, 0.25, 0.1, 0.05, 0.025, 0.01$, and $y_h \ll 1$, plus/or a Comptonization distortion, plus/or a free-free distortion, as described in Sect. 2, in order to analyse the quality of the recovery of the input parameters achievable with the considered experiments.

4 RESULTS

4.1 Fits to simulated data: non distorted spectrum

4.1.1 Analysis in terms of a single spectral distortion

We fit the simulated data set S-BB with a spectrum distorted by a single energy injection at different values of y_h or by a free-free distortion in order to recover the value of $\Delta\epsilon/\epsilon_i$ or of y_B , expected to be null, and the limits (at 95 per cent of CL) on them. The results are reported in Table 1 for a representative set of the considered dissipation epochs. The table shows also the results obtained by using the FIRAS data alone combined with the long wavelength data accumulated in the last two decades (see also Salvaterra & Burigana 2002), the results achievable by combining the FIRAS data with the subset of the data set S-BB achievable by *DIMES* alone (see also Burigana & Salvaterra 2003), and, finally, the results achievable by exploiting the subset of data set S-BB achievable by FIRAS II alone.

The sensitivities reported in Table 1 for a given distortion parameter apply in the case in which quite strong priors can be assumed on the other two distortion parameters. In any case, FIRAS II alone or *DIMES* alone either is able to improve by more than one order of magnitude the current limits on the free-free distortions and on the energy exchanges. It is evident from the table that in this case FIRAS II alone is able to provide the best constraints on the energy exchanges (with a sensitivity improvement by a factor ~ 100) while *DIMES* alone is able to provide the best constraints on the free-free distortions (with a sensitivity improvement by a factor $\simeq 500$), without any significant improvement from the combination of the two experiments.

4.1.2 Joint analysis of three kinds of spectral distortions

We discuss here the possibility to significantly improve the constraints on the spectral distortion parameters in the more general case of a joint analysis of an early/intermediate dissipation process occurred at a given y_h , of a late dissipation process ($y_h \ll 1$), and of a free-free distortion. We exploit the same data sets of the previous subsection but without any prior on the distortion parameters.

The results are reported in Table 2 (95 per cent CL) for a representative set of the earlier dissipation epoch y_h and displayed in Fig. 1 for the whole range of y_h .

| Data set | $(\Delta\epsilon/\epsilon_i)/10^{-7}$ | | | | $y_B/10^{-7}$ |
|----------|---------------------------------------|---------------------------|---------------------------|---------------------------|-----------------------------------|
| | heating at $y_h = 5$ | heating at $y_h = 1.5$ | heating at $y_h = 0.5$ | heating at $y_h \ll 1$ | free-free dist. at $y_h \ll 1$ |
| F | 20±533 | 25±453 | 25±359 | 28±233 | 272±920 |
| F + R | 64±532 | 39±453 | 28±359 | 28±233 | -455±424 |
| D + F | -1.92±18.12 | -4.5±38.1 | -3.2±106.9 | 3.08±210 | -0.02±0.88 |
| F-II | 1.28±3.95 | 1.06±3.35 | 0.83±2.66 | 0.60±2.08 | -3.26±7.33 |
| D + F-II | 1.13±3.85 | 1.02±3.34 | 0.82±2.66 | 0.60±2.08 | -0.07±0.87 |

Table 1. Fits to a single spectral distortion by considering different sets of real and/or simulated data. F: FIRAS; R: recent measures at $\lambda \gtrsim 1$ cm; D: *DIMES*; F-II: FIRAS II. An underlying blackbody spectrum is here assumed for the simulated data sets.

Clearly, the sensitivities on each distortion parameter are worse than the “analogous” one in Table 1, but the relative improvements with respect to the current observational status are similar.

Although FIRAS II (*DIMES*) still plays the most relevant role for the energy exchanges (for the free-free distortions), it is interesting to note that in this case the spectral distortion parameter recovery appreciably improves by combining the two experiments. This is because such levels of accuracy on a so wide frequency range allow to remove the approximate degeneracy both between free-free and BE-like distortions and between Comptonization and BE-like distortions that remain in presence of future significant improvements only at $\lambda \gtrsim 1$ cm or at $\lambda \lesssim 1$ cm, respectively.

This point will be discussed again in the next subsections, where the analysis of the capability of such experiments to measure spectral distortions possibly present in the CMB spectrum and the corresponding dissipation epochs is presented.

4.2 Fits to simulated data: distorted spectra

In this subsection we exploit the simulated data S-E5C, S-E1.5C, and S-E0.1C (see Sect. 3.2) to evaluate the quality of spectral distortion parameter recovery achievable with the considered experiments.

4.2.1 Combining *DIMES* and FIRAS II

We first consider the information achievable by combining *DIMES* and FIRAS II.

In the case of the data set S-E5C, a fit in terms of two energy exchanges at the epochs assumed in the input model ($y_h = 5$ and $y_h \ll 1$) shows that the values of $\Delta\epsilon/\epsilon_i$ can be accurately recovered: for example, in the considered test, we find $\Delta\epsilon/\epsilon_i(y_h = 5) = (2.79 \pm 0.79) \times 10^{-6}$ and $\Delta\epsilon/\epsilon_i(y_h \ll 1) = (3.03 \pm 0.42) \times 10^{-6}$ (errors at 95 per cent CL) with a $\chi^2/\text{d.o.f.} = 1.100$. This results are not significantly affected by allowing also for a free-free distortion. We find in this case: $\Delta\epsilon/\epsilon_i(y_h = 5) = (2.71 \pm 0.90) \times 10^{-6}$, $\Delta\epsilon/\epsilon_i(y_h \ll 1) = (3.06 \pm 0.47) \times 10^{-6}$, and the recovered $y_B = (-1.69 \pm 9.96) \times 10^{-8}$ is clearly in agreement with the null input value ($\chi^2/\text{d.o.f.} = 1.119$).

We verified also that a (wrong) interpretation of these simulated data in terms of a single kind of spectral distortion is clearly ruled out (and the recovery of the spectral distortions parameters is, of course, wrong). Even in the most favourite case of a Comptonization distortion we find a $\chi^2/\text{d.o.f.} \simeq 2$ (the χ^2 goes from $\simeq 58$ of previous fits to $\simeq 108$). Analogously, an interpretation in terms of a single energy dissipation plus a free-free distortion is ruled out (we find $\chi^2/\text{d.o.f.} = 1.774$ in the most favourite case of a Comptonization distortion coupled to a free-free distortion).

We then tried to estimate the epoch of the earlier energy injection. By assuming $y_h = 2$ we find a $\chi^2 \simeq 58$ but a degraded spectral distortion parameter recovery. In particular, the $\Delta\epsilon/\epsilon_i$ value of the later process is very weakly affected, while that of the earlier process is underestimated of $\simeq 10\%$ and a (wrong) small negative free-free detection, $y_B = (-7.34 \pm 9.21) \times 10^{-8}$, appears, although clearly compatible with the input value $y_B = 0$ at $\sim 1.6\sigma$.

If we try a fit assuming $y_h = 1$ the results, substantially unchanged in terms of χ^2 , degrades further from the physical point of view: we find $y_B = (-1.14 \pm 0.89) \times 10^{-7}$, i.e. a sign no longer compatible (at $\simeq 2.6\sigma$) with that of the, again only slightly affected, recovered Comptonization distortion.

| Data set | $(\Delta\epsilon/\epsilon_i)/10^{-7}$ | | | | $y_B/10^{-7}$ |
|----------|---------------------------------------|---------------------------|---------------------------|---------------------------|-----------------------------------|
| | heating at $y_h = 5$ | heating at $y_h = 1.5$ | heating at $y_h = 0.5$ | heating at $y_h \ll 1$ | free-free dist. at $y_h \ll 1$ |
| F | 414±1561 | | | -85±546 | 635±1531 |
| F | | 353±1334 | | -88±560 | 614±1473 |
| F | | | 286±1091 | -99±601 | 583±1392 |
| F + R | -465±1056 | | | 163±436 | -540±469 |
| F + R | | -418±922 | | 176±452 | -542±459 |
| F + R | | | -343±789 | 189±492 | -521±453 |
| D + F | -25.6±56.02 | | | 68.51±231 | -1.12±2.64 |
| D + F | | -35.0±89.1 | | 71.6±240 | -0.67±1.94 |
| D + F | | | -33.6±176.4 | 63.5±275 | -0.14±1.18 |
| F-II | -3.43±13.87 | | | 1.82±6.20 | -5.22±12.06 |
| F-II | | -3.05±12.22 | | 1.92±6.56 | -5.14±11.77 |
| F-II | | | -2.64±10.28 | 2.13±7.15 | -5.03±11.24 |
| D + F-II | 0.51±9.07 | | | 0.36±4.72 | -0.38±1.00 |
| D + F-II | | 0.71±8.00 | | 0.20±4.94 | -0.44±0.90 |
| D + F-II | | | 0.68±6.85 | 0.10±5.42 | -0.54±0.88 |

Table 2. Fits to three kinds of spectral distortions, jointly considered, for different real and/or simulated data. F: FIRAS; R: recent measures at $\lambda \gtrsim 1$ cm; D: *DIMES*; F-II: FIRAS II. An underlying blackbody spectrum is here assumed for the simulated data sets.

To verify the physical trouble of such possible sign differences we computed the (negative) Comptonization distortion parameter produced by simple thermal histories (namely, with $\phi \simeq \text{constant}$ and fully ionized medium) at pre-recombination epochs or after the recombination able to generate free-free distortions in the range on the negative values found above. For example, we find $u \lesssim -1.8 \times 10^{-5}$ by assuming a process in the redshift range $10^4 - 10^3$ and $u \lesssim -5.6 \times 10^{-7}$ for a process in the redshift range $10^3 - 10^2$, while a process in the redshift range $30 - 0$ can produce such negative free-free distortions only for unphysical matter cooling processes involving $\phi \lesssim 0.2$. Since also a cooling process with significant ionization at $z \sim 10^3 - 10^2$ seems to be excluded by *WMAP*, the only possible scenarios producing different signs of y_B and u should involve or a pre-recombination cooling process able to produce negative Comptonization and free-free distortions followed by a late heating process with a very small free-free distortion and a significant Comptonization distortion able to properly compensate the previous one, or, in general, particularly ad hoc thermal histories. In general, these possible scenarios should involve accurate fine tunings and appear difficult and untenable and should be discarded in favour of an early energy injection at relevant y_h followed by a late dissipation mechanism.

In spite of the insignificant variations of the χ^2 , the disagreement between the signs of free-free and Comptonization distortions due to the wrong assumption on the earlier process epoch, tends to “physically” support the (right) interpretation of the S-E5C data set involving an energy dissipation at y_h certainly larger than 1 and, probably, larger than 2 or 3. We then conclude that reliable estimates of the epochs of the possible dissipation processes are achievable by combining *DIMES*-like and FIRAS II-like experiments, even for very small energy exchanges.

By exploiting the data set S-E1.5C, we find that a fit in terms of two energy exchanges at the epochs assumed in the input model ($y_h = 1.5$ and $y_h \ll 1$) allows to recover the values of $\Delta\epsilon/\epsilon_i$ with a sensitivity similar to that quoted above for the data set S-E5C. Again, allowing for a free-free distortion does not represent a problem and models involving a single kind of spectral distortion or a single energy dissipation plus a free-free distortion can be easily ruled out by simple χ^2 arguments. Concerning the determination of the epoch of the earlier energy injection, in this case the comparison between the recovered signs of Comptonization and free-free distortions does not play a relevant role and the direct analysis of the χ^2 rules out values of y_h smaller than $\simeq 0.1$.

Finally, we analysed the data set S-E0.1C. We note that the differences between a spectrum resulting from a dissipation at $y_h \simeq 0.1$ and that produced by a late ($y_h \ll 1$) process are significantly less evident than those between a spectrum

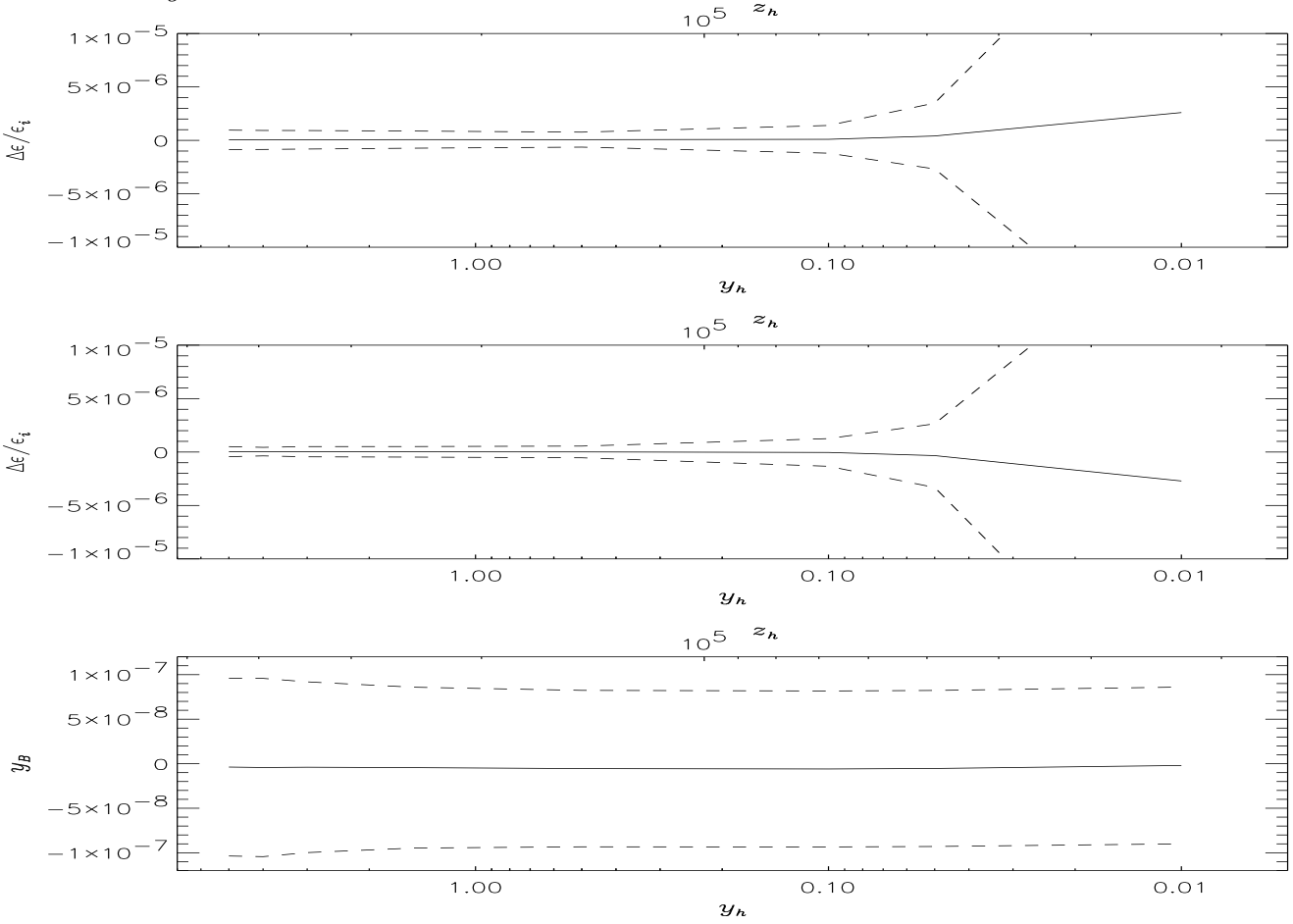


Figure 1. Constraints at 95 per cent CL on two energy exchanges at different epochs and on the free-free distortion, jointly considered, as could be in principle derived by combining a *DIMES*-like experiment with a FIRAS II-like experiment. An underlying blackbody spectrum is here assumed. Solid lines: best fit; dashes: upper and lower limits. Top panel: constraints on $\Delta\epsilon/\epsilon_i(y_h)$ allowing for a later energy exchange at $y_h \ll 1$ and for a free-free distortion. Middle panel: constraints on $\Delta\epsilon/\epsilon_i(y_h \ll 1)$ allowing for a previous energy exchange occurring at y_h and for a free-free distortion. Bottom panel: constraints on y_B allowing for a first energy exchange occurring at y_h and a second energy exchange at $y_h \ll 1$. See also the text.

resulting from a dissipation at relevant y_h ($y_h \gtrsim 1$) and that produced by a late ($y_h \ll 1$) process. Consequently, we may expect a degradation of the fit result quality. In fact, we find an appreciable underestimation of the earlier energy dissipation and an analogous overestimation of the later energy dissipation, and error bars significantly larger than in the previous cases: $\Delta\epsilon/\epsilon_i(y_h = 0.1) = (2.31 \pm 1.34) \times 10^{-6}$ and $\Delta\epsilon/\epsilon_i(y_h \ll 1) = (3.59 \pm 1.33) \times 10^{-6}$ (errors at 95 per cent CL). Note that, even in this unfavourable case, the recovered values of $\Delta\epsilon/\epsilon_i$ are in agreement with the input ones at $\simeq 1\sigma$ level. Also in this case, allowing for a free-free distortion does not degrade further the fit energy exchange recovery and models involving a single kind of spectral distortion or a single energy dissipation plus a free-free distortion can be directly ruled out by simple χ^2 arguments. A firm estimate of the epoch of the earlier energy injection can not be achieved in this case: fits involving models with an earlier energy injection at $y_h \gtrsim 1$ do not show a significant increase of the χ^2 . On the other hand, from the analysis of the previous cases we know that the epoch of a possible energy injection at relevant y_h can be quite well estimated from such high quality data. Therefore, in the situation in which a fit to the data in terms of two energy injections at different epochs (plus, possibly a free-free distortion) does not allow to estimate the epoch of the earlier process, it is quite reasonable to argue that the earlier process has been occurred at an epoch not particularly early (by looking at the results found for the data set S-E1.5C, we argue in this case an upper limit $y_h \lesssim 1$).

We conclude that the combined information contained in future *DIMES* and FIRAS II experiments will allow to clearly identify the presence of spectral distortions also in the quite general case of a thermal histories involving early/intermediate and late processes, to measure the corresponding parameters with a good precision even for small amounts ($\Delta\epsilon/\epsilon_i \sim 10^{-6}$) of dissipated energy, and to quite well constrain the epochs at which the processes have been possibly occurred.

4.2.2 FIRAS II alone

In the previous subsection we have considered the information achievable by combining *DIMES* and FIRAS II. Burigana & Salvaterra 2003 discussed the scientific capabilities of accurate long wavelength measures coupled to the available FIRAS data. We then report here the results obtained by repeating the same analyses carried out above, but by considering the subsets of the data sets S-E5C, S-E1.5C, and S-E0.1C achievable by using FIRAS II alone.

In the case of the data set S-E5C, we find that the two values of $\Delta\epsilon/\epsilon_i$ can be recovered with an accuracy only slightly degraded with respect to that of the previous section only by performing the fit in terms of two energy exchanges at the epochs assumed in the input model (the resulting $\chi^2/\text{d.o.f.} = 1.136$ in this case) while allowing for a free-free distortion implies a degradation of a factor $\simeq 1.5$ in the $\Delta\epsilon/\epsilon_i$ recovery sensitivity. Models with a single spectral distortions can be again ruled out; the same holds for models involving a single energy dissipation plus a free-free distortion, although with a χ^2 increase less significant than that found in the previous subsection (for example, for a fit in terms of a Comptonization distortion coupled to a free-free distortion we find $\chi^2/\text{d.o.f.} = 1.399$, to be compared with the value of 1.774 found in the previous subsection).

Results similar to those described above are found by considering the data set S-E1.5C. The main difference concerns the impact of free-free distortion: by allowing for it in the fit we find in the test a significant underestimation ($\simeq 36\%$, no longer compatible at 1σ with the input one) on the recovery of the earlier energy injection ($\Delta\epsilon/\epsilon_i(y_h = 1.5) = (1.92 \pm 1.35) \times 10^{-6}$) and a corresponding (false) detection of a negative (at $\simeq 1.3\sigma$) free-free distortion ($y_B = (-0.823 \pm 1.248) \times 10^{-6}$) [while the effect on Comptonization distortions is small; we find $\Delta\epsilon/\epsilon_i(y_h \ll 1) = (3.37 \pm 0.72) \times 10^{-6}$, errors at 95 per cent CL]. Clearly, by using only high frequency data, the two errors tends to compensate each other, because of their signatures in the final spectrum.

The exploitation of the data set S-E0.1C shows analogous results. The above problem related to the impact of free-free distortion is further enhanced and the parameter recovery sensitivity is significantly degraded: we find $\Delta\epsilon/\epsilon_i(y_h = 0.1) = (1.58 \pm 2.28) \times 10^{-6}$, $y_B = (-0.517 \pm 1.199) \times 10^{-6}$, $\Delta\epsilon/\epsilon_i(y_h \ll 1) = (4.18 \pm 2.20) \times 10^{-6}$ (errors at 95 per cent CL). In addition, while models with a single spectral distortions can be again directly ruled out, and the same holds for models without a late energy injection, models involving a single late ($y_h \ll 1$) energy dissipation plus a free-free distortion can not be longer ruled out on the basis on a direct χ^2 analysis but on the requirement of having Comptonization and free-free distortions with the same sign (we recover in this case the values $\Delta\epsilon/\epsilon_i(y_h \ll 1) \simeq (5.78 \pm 0.22) \times 10^{-6}$, i.e. about corresponding to the sum the energy dissipated by the two processes in order to fit the higher frequency tail of the spectrum, and a negative y_B ($\simeq (-1.22 \pm 0.76) \times 10^{-6}$) that tends to mimic the effect of an earlier energy dissipation).

Finally, we find that for all the three data sets only a poor information on the epoch of the earlier energy dissipation can be achieved.

4.2.3 FIRAS II alone versus DIMES and FIRAS II

From the comparison between the results reported in the two previous subsections we can draw the following conclusions.

A FIRAS II-like experiment shows a sensitivity to the values of the two energy exchanges at different cosmic times similar to that achieved by combining a FIRAS II-like experiment and a *DIMES*-like experiment only in presence of a strong prior on the free-free distortion.

In the realistic case in which also y_B should be recovered from the CMB spectrum data, the sensitivity of the spectral distortion parameter recovery will result significantly affected with respect to the case in which both FIRAS II and a *DIMES* data are available, with a sensitivity degradation factor of about 1.5–2, related to the epoch of the earlier dissipation process, and possible significant deviations of the recovered values from the input ones.

In addition, the rejection of “wrong” (i.e. different from those assumed in the input model) models becomes less reliable in the case of earlier dissipations at $y_h \sim \text{some} \times 0.1$, being based no longer on direct χ^2 analyses but on physical requirements about the signs of the recovered free-free and Comptonization distortions.

Finally, quite accurate estimates of the epochs of the earlier processes are no longer possible.

By combining these results with those reported in Sect. 4.1 and with those presented in Burigana & Salvaterra 2003, we conclude that, although a significant progress of CMB spectrum measures only at $\lambda \gtrsim 1$ cm or at $\lambda \lesssim 1$ cm certainly implies a great improvement of the current knowledge of thermal history of the Universe, only the combination of very precise measures both at $\lambda \gtrsim 1$ cm and at $\lambda \lesssim 1$ cm will allow to recover the spectral distortion parameters and to map the thermal history of the Universe under quite general conditions.

4.3 Constraints on very high redshift processes

We extend here at $z_h > z_1$ (i.e. $y_h > 5$) the constraints on $\Delta\epsilon/\epsilon_i$ that would be possible to derive at $z_h = z_1$ ($y_h = 5$) with the combination of a *DIMES*-like and a FIRAS II-like experiment. We remember that at $z > z_1$ the Compton scattering is able to restore, after an energy injection, the kinetic equilibrium between matter and radiation, yielding a BE spectrum, and the

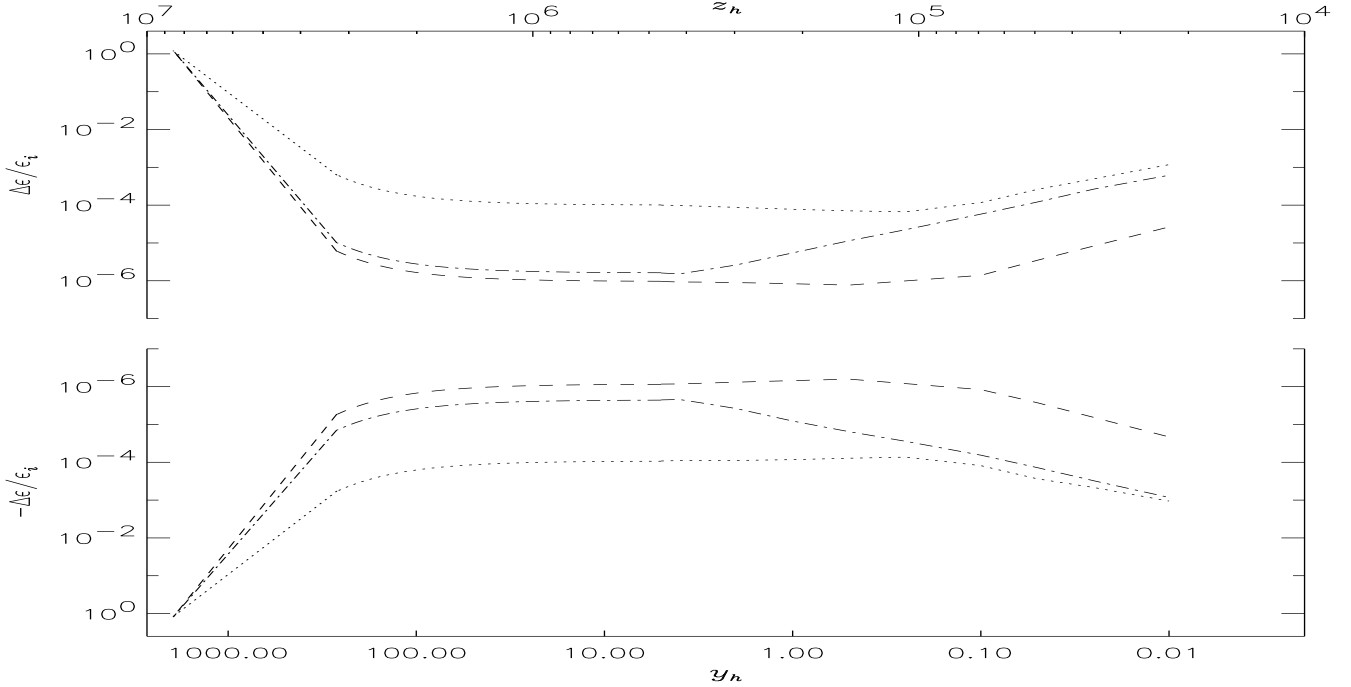


Figure 2. Comparison between the constraints on the energy exchanges derived from current measures – FIRAS and long wavelength data – (dotted lines; in practice FIRAS data alone set the current constraints, see Salvaterra & Burigana 2002), from FIRAS data jointed to a simulated data set from a *DIMES*-like experiment (dash-dotted lines; see Burigana & Salvaterra 2003), and, finally, from simulated data sets from a *DIMES*-like experiment jointed to a FIRAS II-like experiment (dashed lines). An underlying blackbody spectrum is here assumed for the simulated data sets. In the first two cases (dotted lines and dash-dotted lines) we report the constraints on $\Delta\epsilon/\epsilon_i(y_h)$ allowing for a later energy exchange at $y_h \ll 1$ but neglecting free-free distortions (i.e. assuming $y_B = 0$). In the last case (dashed lines) we relax the assumption $y_B = 0$, i.e. we jointly consider three kinds of spectral distortions. See also the text.

combined effect of Compton scattering and photon production processes tends to reduce the magnitude of spectral distortions, possibly leading to a blackbody spectrum. The contribution to the thermalization process by a possible cyclotron emission associated to cosmic magnetic fields by including also stimulated emission and absorption (Afshordi 2002 and references therein) has been recently evaluated for realistic shapes of the distorted spectrum at early epochs (Zizzo 2003, Zizzo & Burigana 2003): the strong decreasing of the frequency dependent chemical potential, $\mu(x)$, of the BE-like spectrum (Sunyaev & Zeldovich 1970) at the very long wavelengths relevant for the cyclotron process implies a large suppression of the cyclotron efficiency. Therefore, only for values of the cosmic magnetic field, B , larger than $\approx 10^{-6}$ G, well above current observational evidences and theoretical predictions, this process is found to play a significant role, comparable to (or larger than) the combined effect of radiative Compton and bremsstrahlung that drives the thermalization process for reasonable values of B .

We consider here for simplicity only the case of the simulated observation of a not distorted spectrum, that represents a good example of the possible improvements represented by such kinds of experiments, directly comparable to the results based on the current data. The comparison is shown in Fig. 2, where the results obtained by considering only simulated data from a *DIMES*-like experiment together with the real FIRAS data (Burigana & Salvaterra 2003) are also reported.

Note how the constraints on $\Delta\epsilon/\epsilon_i$ can be improved by a factor $\sim 10 - 100$ for processes possibly occurred in a wide range of cosmic epochs, corresponding to about a decade in redshift at z about 10^6 .

It is also evident the improvement of the constraints on $\Delta\epsilon/\epsilon_i$ at $z_h \lesssim \text{few} \times 10^5$, possible by adding FIRAS II data to *DIMES* data.

Finally, note that the results based on simulated FIRAS II and *DIMES* data are obtained by relaxing any assumption on y_B , assumed to be null in the other two cases (compare also the different cases reported in Tables 1 and 2).

Of course, large energy injections are still possible at very early epochs close to the thermalization redshift, when primordial nucleosynthesis set the ultimately constraints on energy injections in the cosmic radiation field.

5 IMPLICATIONS FOR SOME CLASSES OF LATE ASTROPHYSICAL PROCESSES

In the previous sections the constraints on free-free and Comptonization distortions from the new generation of CMB spectrum experiments have been considered from a general point of view, without assuming detailed physical models for their genesis. Such kinds of late distortions are expected in many astrophysical scenarios involving some energy dissipation mechanisms during various stages of the star and galaxy evolution or some particle or scalar field decay model (see e.g. De Zotti & Burigana 1992, Tegmark & Silk 1995). The relevance of their detection (Kogut 2003) has been partially renewed by the *WMAP* satellite discovery of a reionization phase at relevant redshifts, mainly supported by *WMAP* detection of an excess in the CMB TE cross-power spectrum on large angular scale (multipoles $\ell \lesssim 7$), indicating an optical depth to the CMB last scattering surface of $\tau_e \simeq 0.16$ (Kogut et al. 2003).

Without the ambition to exhaustively cover a so wide topic, we compare here the coupled free-free and Comptonization distortions for some of the models recently discussed in the literature and discuss the possibility to reveal them with the new generation of CMB spectrum experiments.

Table 3 summarizes the chances of observing the Comptonization and free-free distortions for the four classes of processes discussed in the following subsections on the basis of the sensitivities reported in Table 2 (of course, a more optimistic conclusion for the possibility to measure the Comptonization distortion, i.e. a sensitivity improvement by a factor $\simeq 2.5 - 3$, could be derived by assuming a quite strong prior on the earlier energy exchange; compare the last row of Table A1 with the last three rows of Table 2).

5.1 Free-free emitters

Oh (1999) predicted the level of free-free distortion can be produced by ionized halos in the early stage of galaxy formation by computing the moments of the intensity distribution from a Press-Schechter based model. The predicted free-free distortion results to be $\Delta T_B = 3.4 \times 10^{-3}$ K at $\simeq 2$ GHz corresponding to a free-free distortion parameter $y_B \simeq 1.5 \times 10^{-6}$, well within the sensitivity of *DIMES*. The associated Comptonization distortion predicted in this work is below the current FIRAS upper limit by about one order of magnitude, and is then likely measurable by a FIRAS II-like experiment. Moreover, this work assumed that free-free emitters are the only radio-bright sources in the sky. The existence of radio-loud galaxies and AGNs is likely to increase the spectral distortion due to radio sources.

5.2 Quasar driven blastwaves

The integrated Comptonization distortion from quasar driven blastwaves has been recently computed by Platania et al. 2002 through a quite general “energetic” approach, not particularly related to a detailed physical assumption. They found $u \approx 2.4 \times 10^{-6}$, clearly measurable with a FIRAS II-like experiment, with approximately the same fractional contribution from low- z (0–2) and high- z (2–4) objects. The evaluation of the corresponding integrated free-free distortion is less model independent, being significantly sensitive to the density profile inside the blastwave because of the n_e^2 dependence of the free-free emission. By assuming the model described in Sect. 2 of Platania et al. 2002, we have computed the ratio between the Comptonization parameter u and the free-free parameter y_B integrated over the line-of-sight of the blastwave centre between the galaxy outer cut-off radius, R_g , approximately separating the virialized and infall regions, and an inner radius, r_{ff} ($\approx (1/10 - 1/20) \times R_g$, where the time required for the shock front to reach the outer radius of the galaxy equals the free-free cooling timescale (it is in fact reasonable to assume that the physical conditions at $r < r_{ff}$ are more related to the central engine than to the blastwave evolution). By assuming an electron temperature $T_e \sim 10^6$ K ($T_e \sim 10^7$ K) and a wide range of line-of-sight velocity dispersions, $\sigma \sim 100 - 400$ Km/s, we find $y_B/u \lesssim \text{few} \times 10^{-2}$ ($\lesssim \text{few} \times 10^{-3}$) for objects both at $z \sim 1$ and at $z \sim 3$, while only for low values of T_e ($\sim 10^5$ K) and high values of σ (~ 400) y_B/u approaches the unity. A reasonable upper limit to y_B in this model is then $\sim \text{some} \times 10^{-8} - 10^{-7}$, a value significantly smaller than the free-free distortion predicted in the model by Oh 1999 and below or comparable to the sensitivity of a *DIMES*-like experiment.

5.3 First stars in galaxies

The reionization of the Universe indicated by the *WMAP* data must have begun at relatively high redshift. Ciardi, Ferrara & White (2003) have studied the reionization process using supercomputer simulations of a large and representative region of a Universe which has cosmological parameters consistent with the *WMAP* results. The simulation follows both the radiative transfer of ionizing photons and the formation and evolution of the galaxy population which produces them.

They have shown that the *WMAP* measured optical depth to electron scattering is easily reproduced by a model in which reionization is caused by the first stars in galaxies with total masses of a few $\times 10^9 M_\odot$. Moreover, the first stars are “normal objects”, i.e. their mass is in the range $1-50 M_\odot$, but metal-free. Among the different model explored, the “best” *WMAP* value for τ_e is matched assuming a moderately top-heavy initial mass function (IMF) (Larson IMF with $M_c = 5 M_\odot$) and an

| Process | Comptonization distortion (mainly through FIRAS II) | Free-free distortion (mainly through <i>DIMES</i>) |
|---------|--|--|
| FFE | measurable | measurable |
| QSOB | measurable | \approx at limit |
| FSG | measurable | unobservable |
| PD | measurable | observable |

Table 3. Chances to observe or quite accurately measure Comptonization and free-free distortions with the new generation of CMB spectrum space experiments for some classes of processes. FFE: free-free emitters; QSOB: quasar driven blastwaves; FSG: first stars in galaxies; PD: particle decay. Clearly, the combined effect of these (and, of course, many others) processes should be carefully evaluated and, at least for the astrophysical models, the “integrated” information contained in the CMB spectrum should be hopefully complemented by (or, viceversa, should complement the) dedicated observations (or, at least, detections) of the corresponding astrophysical sources and, possibly, foreground fluctuation analyses. Anyway, these examples show how the combined information of accurate CMB spectrum measures at short and long wavelengths can greatly improve the reliability of a physical explanation of a possible observation of a given kind of spectral distortion.

escape fraction of 20%. A Salpeter IMF with the same escape fraction gives $\tau_e = 0.132$, which is still all the suggested 68% confidence ranges. Decreasing f_{esc} to 5% gives $\tau_e = 0.104$, which disagrees with *WMAP* only at $\simeq 1.0 - 1.5\sigma$ level, the exact level depending on the detailed cosmological scenario adopted to fit the *WMAP* (and auxiliary) data.

Using the redshift evolution of the density of free electrons obtained by these simulations (kindly provided us by A. Ferrara), we compute the expected CMB spectral distortions. We obtain u -distortions of the order of 2.3×10^{-6} (4.5×10^{-7}) for a constant electron temperature of 10^6 K (2×10^4 K) corresponding to an energy injection of $\Delta\epsilon/\epsilon_i \sim 9.2 \times 10^{-6}$ (1.8×10^{-6}) well below the current FIRAS upper limits, but easily detectable by an experiment with a sensitivity such that proposed for FIRAS II. We compute also the corresponding free-free distortion that results to be so small ($y_B \sim 10^{-11}$) that can not be detected by any future experiment.

In the best-fit model of Ciardi et al. (2003) reionization is essentially complete by $z_r \simeq 13$. This is difficult to reconcile with observations of the Gunn-Peterson effect in $z > 6$ quasars (Becker et al. 2001; Fan et al. 2002). This implies a volume-average neutral fraction above 10^{-3} and a mass-averaged neutral fraction $\sim 1\%$ at $z = 6$. A fascinating (although speculative) possibility is that the Universe was reionized twice (Cen 2003; Whyte & Loeb 2002) with a relatively short redshift interval in which the IGM became neutral again.

5.4 Particle decays

An alternative scenario has been proposed by Hansen & Haiman (2003). They considered the case of a cosmologically significant particle with the property that it decays around a redshift $z \sim 20$. The decay products could have energies high enough to reionize the light elements. If this hypothetical particle is sufficient abundant, then it may explain the high value of the optical depth, without the need for stars to reionize the Universe at high redshift, but normal stellar populations could form at $z \lesssim 10$ with the usual efficiencies and account for the completion of reionization epoch that appears to be occurring at $z < 10$.

Hansen & Haiman (2003) proposed that this particle could be a sterile neutrino with a mass $m_\nu \sim 200$ MeV and decay time $\tau_d \sim 4 \times 10^{15}$ s. The decaying of this neutrino can account for the electron scattering optical depth $\tau \simeq 0.16$ (Kogut et al. 2003) measured by *WMAP* without violating existing astrophysical limits on the CMB and gamma ray background. In particular, they have shown that the expected energy injection in the CMB of this process is $\Delta\epsilon/\epsilon_i \sim 0.4 - 3 \times 10^{-6}$, depending on the fraction of the mean electron energy that goes into heating the IGM. These values are well below the current FIRAS upper limits, but in principle can be detected by future experiments such as FIRAS II (Fixsen & Mather 2002). We calculate the associated free-free distortion of the CMB spectrum generated during a redshift interval corresponding to a time interval between $\sim \tau_d/10$ and $\sim 3\tau_d$ for different simple thermal histories ($T_e \simeq \text{const}$ or $\phi \simeq \text{const}$) producing the above values of $\Delta\epsilon/\epsilon_i$. The expected y_B is in the range $0.4 - 1.4 \times 10^{-7}$ depending mainly on the exact amount of energy that goes into the IGM and only slightly on the considered thermal history of the process. Particularly for cases in which a large amount of the electron energy goes into heating the IGM, this distortion can be in principle observable by the future *DIMES* experiment.

6 DISCUSSION AND CONCLUSIONS

We have studied the implications of the new generation of CMB spectrum space experiments for our knowledge of the thermal history of the Universe.

The combination of two experiments with the sensitivity and the frequency coverage jointly foreseen for *DIMES* and FIRAS II will be able to greatly change our vision of the capability of the CMB spectrum information to constrain physical processes at different cosmic ages. The limits on the energy dissipations at the all cosmic times accessible to CMB spectrum investigations ($z \lesssim z_{therm}$) could be improved by about two order of magnitudes and even dissipation processes with $\Delta\epsilon/\epsilon_i \sim 10^{-6}$ could be detected and possibly accurately studied.

We tested also the possibility to have an independent cross-check on the baryon density accurately measured by CMB anisotropy experiments in presence of possible small early distortions, by using such accurate measures at $\lambda \lesssim 1$ cm to determine the chemical potential and the longer wavelengths to estimate $\hat{\Omega}_b$ through the decreasing of the equivalent thermodynamic temperature at increasing wavelengths, without finding a significant improvement with respect to the results previously described in Burigana & Salvaterra 2003: only high accuracy measures at very long wavelengths (≈ 50 cm) about the minimum of the equivalent thermodynamic temperature are able to provide a firm and accurate independent cross-check on $\hat{\Omega}_b$.

With a joint analysis of two dissipation processes occurring at different epochs, we demonstrated that the sensitivity and the wide frequency range jointly covered by *DIMES* and FIRAS II would allow to accurately recover the two amounts of energy exchanged in the primeval plasma and to constrain quite well also the epochs of the two processes even when possible, a priori unknown, imprints from free-free distortions are taken into account in the data analysis. All the three distortion parameters could be in fact accurately reconstructed in this perspective: the sensitivity at 95 per cent CL is $\simeq (5-9) \times 10^{-7}$ for the two values of $\Delta\epsilon/\epsilon_i$ and of $\simeq 10^{-7}$ for y_B .

These results are possible because such levels of accuracy on a so wide frequency range allow to remove the approximate degeneracy both between free-free and BE-like distortions and between Comptonization and BE-like distortions that remain in presence of future significant improvements only at $\lambda \gtrsim 1$ cm or at $\lambda \lesssim 1$ cm, respectively. The sensitivity on $\Delta\epsilon/\epsilon_i$, mainly determined by a FIRAS II-like experiment, improves by a factor $\simeq 1.5$ by adding the information from a *DIMES*-like experiment, while the sensitivity on y_B , mainly determined by a *DIMES*-like experiment, improves by a factor $\simeq 1.3-2.6$, by adding the information from a FIRAS II-like experiment.

Of course, not only a very good sensitivity, but also an extreme control of the all systematic effects and, in particular, of the frequency calibration is crucial to reach these goals.

Finally, we discussed the different signatures imprinted on the CMB spectrum by some late astrophysical and particle decay models recently proposed in the literature and possibly related to the reionization of the Universe indicated by *WMAP*, and compared them with the sensitivity of such classes of CMB space spectrum experiments. Different processes produce different levels of coupled Comptonization and free-free distortions and the combination of very accurate CMB spectrum measures at long and short wavelengths can in principle probe or constrain these models.

ACKNOWLEDGEMENTS

We warmly thank L. Danese, G. De Zotti, A. Ferrara and P. Platania for numberless conversations on theoretical aspects of CMB spectral distortions and on the ionization history. It is a pleasure to thank M. Bersanelli and N. Mandolesi for useful discussions on CMB spectrum observations. Some of the calculations presented in Sect. 5 have been carried out on an alpha digital unix machine at the IFP/CNR in Milano by using some NAG integration codes.

APPENDIX A: JOINT ANALYSIS OF TWO KINDS OF SPECTRAL DISTORTIONS

For sake of completeness we report in Table A1 the constraints that can be in principle derived from a FIRAS II-like experiment and from the combination of a *DIMES*-like experiment with a FIRAS II-like experiment in the joint analysis of two kinds of spectral distortions. These sensitivities on a couple of distortion parameters apply in the case in which a quite strong prior is assumed on the third distortion parameter (in practice, assuming it ranging within an interval much smaller than the corresponding sensitivity quoted in Table 2). Compare Table A1 with Table 2. Although the best sensitivity on y_B is reached when the earlier energy exchange is assumed known, the sensitivity on y_B does not depend much on the considered case and not much degrades by considering two energy exchanges. Finally, the sensitivity on one of the two energy exchanges is better by assuming known the other one and unknown the free-free distortion than by assuming known the free-free distortion and unknown the other energy exchange.

| Data set | $(\Delta\epsilon/\epsilon_i)/10^{-7}$ | | | | $y_B/10^{-7}$ |
|----------|---------------------------------------|---------------------------|---------------------------|---------------------------|-----------------------------------|
| | heating at $y_h = 5$ | heating at $y_h = 1.5$ | heating at $y_h = 0.5$ | heating at $y_h \ll 1$ | free-free dist. at $y_h \ll 1$ |
| F-II | 1.27±8.84 | | | 0.05±4.66 | |
| F-II | | 1.00±8.02 | | 0.04±4.97 | |
| F-II | | | 0.77±6.97 | 0.04±5.45 | |
| F-II | 0.40±4.83 | | | | -2.83±8.97 |
| F-II | | 0.34±4.03 | | | -2.84±8.81 |
| F-II | | | 0.29±3.11 | | -2.84±8.57 |
| F-II | | | | 0.38±2.16 | -2.91±7.60 |
| D + F-II | 0.67±7.69 | | | 2.84±4.15 | |
| D + F-II | | 0.81±7.60 | | 0.14±4.72 | |
| D + F-II | | | 0.74±7.02 | 0.07±5.48 | |
| D + F-II | 1.13±4.00 | | | | -0.01±0.90 |
| D + F-II | | 1.00±3.38 | | | -0.04±0.88 |
| D + F-II | | | 0.81±2.67 | | -0.05±0.87 |
| D + F-II | | | | 0.60±2.08 | -0.06±0.87 |

Table A1. Fits to two kinds of spectral distortions, jointly considered, for different simulated data. D: *DIMES*; F-II: FIRAS II. An underlying blackbody spectrum is here assumed.

REFERENCES

- Afshordi N., 2002, PRL, submitted, astro-ph/0202082
 Becker R.H. et al., 2001, AJ, 122, 2850
 Bennett C.L. et al., 1996, Amer. Astron. Soc. Meet., 88.05
 Bennett C.L. et al., 2003, ApJ, in press, astro-ph/0302207
 Burigana C., Danese L., De Zotti G., 1991a, A&A, 246, 59
 Burigana C., De Zotti G., Danese L., 1991b, ApJ, 379, 1
 Burigana C., De Zotti G., Danese L., 1995, A&A, 303, 323
 Burigana C. & Salvaterra R., 2000, Int. Rep. ITeSRE/CNR 291/2000, August
 Burigana C. & Salvaterra R., 2003, MNRAS, 342, 543
 Cen R., 2003, ApJ, 591, 12
 Ciardi B., Ferrara A. & White S.M.D., 2003, MNRAS, submitted, astro-ph/0302451
 Danese L. & Burigana C., 1993, *Theoretical aspects of the CMB spectrum*, in “Present and Future of the Cosmic Microwave Background”, Lecture in Physics, Vol. 429, eds. J.L. Sanz, E. Martinez-Gonzales, L. Cayon, Springer Verlag, Heidelberg, FRG, p. 28
 Danese L. & De Zotti G., 1977, Riv. Nuovo Cimento, 7, 277
 De Zotti G. & Burigana C., 1992, *The Cosmic Microwave Background Spectrum: Theoretical Framework*, in “Highlights of Astronomy”, Vol. 9, ed. J. Bergeron, Kluwer Academic Publishers, London, UK, p. 265
 Fan X. et al., 2002, AJ, 123, 1247
 Fixsen D.J. et al., 1994, ApJ, 420, 457
 Fixsen D.J. et al., 1996, ApJ, 473, 576
 Fixsen D.J. & Mather J.C., 2002, ApJ, 581, 817
 Hansen S.H. & Haiman Z., 2003, ApJL, submitted, astro-ph/0305126
 Kogut A., 1996, *Diffuse Microwave Emission Survey*, contribution to the XVI Moriond Astrophysics meeting “Microwave Background Anisotropies”, March 16-23, Les Arcs, France, astro-ph/9607100
 Kogut A., 2003, *Reionization and Structure Formation with ARCADE*, to be published in the proceedings of “The Cosmic Microwave Background and its Polarization”, New Astronomy Reviews, eds. S. Hanany & K.A. Olive, astro-ph/0306044
 Kogut A. et al., 2003, ApJ, in press, astro-ph/0302213
 Kompaneets A.S., 1956, Zh. Eksp. Teor. Fiz., 31, 876 [Sov. Phys. JEPT, 4, 730, (1957)]
 Mandolesi N. et al., 1998, PLANCK LFI, A Proposal Submitted to the ESA
 Mather J.C., Fixsen D.J., Shafer R.A., Mosier C., Wilkinson D.T., 1999, ApJ, 512, 511
 Nordberg H.P. & Smoot G.F., 1998, astro-ph/9805123
 Oh S.P., 1999, ApJ, 527, 16
 Platania P., Burigana C., De Zotti G., Lazzaro E., Bersanelli M. 2002, MNRAS, 337, 242
 Press W.H., Teukolsky S.A., Vetterling W.T., Flannery B.P., 1992, “Numerical Recipes in Fortran”, second edition, Cambridge University Press, USA
 Puget, J.L. et al., 1998, HFI for the PLANCK Mission, A Proposal Submitted to the ESA
 Salvaterra R. & Burigana C., 2000, Int. Rep. ITeSRE/CNR 270/2000, March, astro-ph/0206350
 Salvaterra R. & Burigana C., 2002, MNRAS, 336, 592
 Smoot G.F. et al., 1992, ApJ, 396, L1

Sunyaev R.A. & Zeldovich Ya.B., 1970, Ap&SS, 7, 20

Tauber J.A., 2000, *The PLANCK Mission*, in “The Extragalactic Infrared Background and its Cosmological Implications”, Proceedings of the IAU Symposium, Vol. 204, eds. M. Harwit and M. Hauser

Tegmark M. & Silk J., 1995, ApJ, 441, 458

Whyte S. & Loeb A., 2003, ApJL, in press, astro-ph/0302297

Zeldovich Ya.B. & Sunyaev R.A., 1969, Ap&SS, 4, 301

Zeldovich Ya.B., Illarionov A.F., Sunyaev R.A., 1972, Zh. Eksp. Teor. Fiz., 62, 1216 [Sov. Phys. JEPT, 35, 643]

Zizzo A., 2003, Degree Thesis, Bologna University

Zizzo A. & Burigana C., 2003, in preparation